

An Ultra-Fast MLE for Low SNR Multi-Reference Alignment

Shay Kreymer, Amnon Balanov, and Tamir Bendory

Abstract—Motivated by single-particle cryo-electron microscopy, multi-reference alignment (MRA) models the task of recovering an unknown signal from multiple noisy observations corrupted by random rotations. The standard approach, expectation-maximization (EM), often becomes computationally prohibitive, particularly in low signal-to-noise ratio (SNR) settings. We introduce an alternative, ultra-fast algorithm for MRA over the special orthogonal group $SO(2)$. By performing a Taylor expansion of the log-likelihood in the low-SNR regime, we estimate the signal by sequentially computing data-driven averages of observations. Our method requires only one pass over the data, dramatically reducing computational cost compared to EM. Numerical experiments show that the proposed approach achieves high accuracy in low-SNR environments and provides an excellent initialization for subsequent EM refinement.

Index Terms—Multi-reference alignment, Maximum likelihood estimation, Cryo-electron microscopy

I. INTRODUCTION

THE PROBLEM of estimating a signal from multiple noisy observations, each undergoing an unknown group action, is fundamental in biomedical imaging [1], computer vision [2], and signal processing [3]. This task is formally known as multi-reference alignment (MRA) [4], [5]. In this paper, we focus on the MRA problem over the special orthogonal group $SO(2)$ in highly noisy environments. A prominent application of high-noise MRA is single-particle cryo-electron microscopy (cryo-EM), a Nobel-winning technology for determining the 3D structure of biological macromolecules [6], [7], [8]. In cryo-EM, the goal is to reconstruct a 3D volume from 2D tomographic projection images taken at unknown viewing angles and corrupted by severe noise [9], [10], [11]. While the full reconstruction task involves $SO(3)$ rotations and tomographic projections, the $SO(2)$ MRA model captures the core algorithmic challenge of estimating latent transformations under extreme noise [12], [13]. Consequently, the framework presented in this work lays the algorithmic foundation for the significantly more complex 3D reconstruction problem of cryo-EM; see Section V for further discussion.

In the low-SNR regime, estimating the individual rotation angles is statistically impossible, and the sample complexity is bounded by $n = \omega(\sigma^6)$ ¹ [14], [15], where n is the number of

Shay Kreymer is supported by TAD Excellence Program for Doctoral Students in Artificial Intelligence and Data Science. Tamir Bendory is supported in part by BSF under Grant 2020159, in part by NSF-BSF under Grant 2019752, and in part by ISF under Grant 1924/21. (Corresponding author: Shay Kreymer.)

The authors are with the School of Electrical and Computer Engineering, Tel Aviv University, Tel Aviv 69978, Israel (e-mail: shaykreymer@mail.tau.ac.il, amnonba15@gmail.com, bendory@tauex.tau.ac.il).

¹ $n = \omega(\sigma^6)$ means that $n/\sigma^6 \rightarrow \infty$ as $n, \sigma \rightarrow \infty$.

observations and σ is the standard deviation of the noise. The prevailing approach for solving such problems is maximum likelihood estimation (MLE), typically implemented via the expectation-maximization (EM) algorithm [16], [17]. EM treats the unknown rotations as latent variables, estimating the signal by maximizing the expected log-likelihood with respect to the posterior distribution of these rotations. However, EM suffers from two major drawbacks. First, the likelihood landscape is non-convex, and EM is prone to getting trapped in spurious local minima unless initialized with a high-quality guess [18], [19]. Second, EM is computationally expensive, as it requires multiple iterations over the entire dataset [20]. Alternative approaches based on invariant features [21], [12], [22] provide consistency, but may become computationally challenging in complex settings such as cryo-EM.

In this paper, we introduce a computationally efficient approximation to the MLE that avoids iterative refinement. Leveraging the low-SNR assumption, we linearize the marginalized likelihood to derive a sequential “frequency marching” estimator that propagates phase information from lower to higher frequencies based on data-driven averages of the observations. Our primary contribution is the derivation of this analytic approximation for MRA over $SO(2)$ in the high-noise regime, which yields a single-pass, closed-form algorithm. Furthermore, through numerical experiments (Section IV), we demonstrate that this method achieves performance comparable to EM while substantially reducing running time, and can be utilized to initialize EM for further accuracy refinement.

This work serves as a foundational step, establishing the algorithmic framework of low-SNR likelihood expansion. In Section V, we outline how this approach can be generalized to the full 3D cryo-EM reconstruction problem.

II. MLE ALGORITHM FOR LOW SNR MRA

In this section, we present the mathematical formulation and derivation of our fast MLE algorithm. We begin by defining the MRA model over $SO(2)$ and the likelihood function. We then derive an approximation of the likelihood using a first-order Taylor expansion, justified by the low-SNR assumption. Finally, based on this approximation, we introduce a frequency-marching algorithm, which recovers the Fourier coefficients sequentially in a closed form.

A. Statistical model

We consider a real bandlimited signal on the unit circle:

$$f(t) = \sum_{k=-L}^L \hat{f}[k] e^{ikt}, \quad t \in [0, 2\pi), \quad (1)$$

where L is the bandlimit of the signal. Since f is real, its Fourier transform is conjugate symmetric, i.e., $\hat{f}[-k] = \hat{f}[k]$. For an angle $\theta \in [0, 2\pi)$, the rotation operator $R_\theta \in \text{SO}(2)$ is defined by

$$(R_\theta f)(t) = f(t - \theta) = \sum_{k=-L}^L \hat{f}[k] e^{-ik\theta} e^{ikt}. \quad (2)$$

We consider a set of n observations,

$$y_j = R_{\theta_j} f + \varepsilon_j, \quad j = 1, \dots, n, \quad (3)$$

where $\varepsilon_j \stackrel{\text{i.i.d.}}{\sim} \mathcal{N}(0, \sigma^2 I)$, and $\theta_j \stackrel{\text{i.i.d.}}{\sim} \text{Unif}[0, 2\pi)$. The assumption that the distribution over the angles is uniform is unnecessary, and we take it only for simplicity. In the Fourier domain, the observations satisfy

$$\hat{y}_j[k] = \hat{f}[k] e^{-ik\theta_j} + \hat{\varepsilon}_j[k], \quad (4)$$

where $\hat{\varepsilon}_j \stackrel{\text{i.i.d.}}{\sim} \mathcal{CN}(0, \sigma^2 I)$. We note that the signal can be estimated only up to a global rotation.

B. Preliminary estimates

The algorithm begins with the estimation of the zero-frequency component $\hat{f}[0]$ (requires $n = \omega(\sigma^2)$ observations)

$$\widehat{\hat{f}[0]} = \frac{1}{n} \sum_{j=1}^n \hat{y}_j[0], \quad (5)$$

and the Fourier magnitudes $|\hat{f}[k]|$ (requires $n = \omega(\sigma^4)$ observations)

$$\widehat{|\hat{f}[k]|} = \sqrt{\frac{1}{n} \left(\sum_{j=1}^n |\hat{y}_j[k]|^2 - \sigma^2 \right)}. \quad (6)$$

Using these estimates, and due to the conjugate symmetry, it is enough to consider frequencies $k = 1, \dots, L$.

C. Conditional likelihood

To break the inherent rotational symmetry of the MRA problem, we arbitrarily fix the phase of the $k = 1$ coefficient by setting $\hat{f}[1] = |\hat{f}[1]|$. With this anchor established, we aim to maximize the log-likelihood of the k -th Fourier coefficient phase, conditioned on the estimates of the other frequencies $\{k' \in [0, L] : k' \neq k\}$:

$$\begin{aligned} \ell(\hat{f}[k]; \{\hat{f}[k']\}_{k'=0, k' \neq k}^L) &:= \ell(\hat{f}[k]) \\ &= \sum_{j=1}^n \log \int_{\theta=0}^{2\pi} \frac{1}{(2\pi\sigma^2)^{L/2}} e^{\frac{-1}{2\sigma^2} \sum_{m=0}^L |\hat{y}_j[m] - \hat{f}[m]|^2 - im\theta} d\theta. \end{aligned} \quad (7)$$

To simplify the expression, we expand the least squares term in the exponent:

$$\begin{aligned} -\frac{1}{2\sigma^2} \sum_{m=0}^L |\hat{y}_j[m] - \hat{f}[m]|^2 &= -\frac{1}{2\sigma^2} \|\hat{y}_j\|_2^2 - \frac{1}{2\sigma^2} \|\hat{f}\|_2^2 \\ &+ \frac{1}{\sigma^2} \sum_{k' \neq k} \Re \bar{\hat{y}}_j[k'] \hat{f}[k'] e^{-ik'\theta} + \frac{1}{\sigma^2} \Re \bar{\hat{y}}_j[k] \hat{f}[k] e^{-ik\theta}, \end{aligned} \quad (8)$$

and rewrite

$$\begin{aligned} \ell(\hat{f}[k]) &= \sum_{j=1}^n \log \int_{\theta=0}^{2\pi} \frac{1}{(2\pi\sigma^2)^{L/2}} e^{\frac{-1}{\sigma^2} \Re \bar{\hat{y}}_j[k] \hat{f}[k] e^{-ik\theta}} \\ &\quad e^{-\frac{1}{2\sigma^2} \|\hat{y}_j\|_2^2 - \frac{1}{2\sigma^2} \|\hat{f}\|_2^2 + \frac{1}{\sigma^2} \sum_{k' \neq k} \Re \bar{\hat{y}}_j[k'] \hat{f}[k'] e^{-ik'\theta}} d\theta \\ &= \sum_{j=1}^n \log C_1 \int_{\theta=0}^{2\pi} e^{\frac{1}{\sigma^2} \Re \bar{\hat{y}}_j[k] \hat{f}[k] e^{-ik\theta}} e^{C_{j,k}(\theta)} d\theta, \end{aligned} \quad (9)$$

where

$$C_{j,k}(\theta) := \frac{1}{\sigma^2} \sum_{k' \neq k} \Re \bar{\hat{y}}_j[k'] \hat{f}[k'] e^{-ik'\theta}, \quad (10)$$

and C_1 is a constant. The first exponent admits the second-order Taylor expansion in powers of $\|\hat{f}\|/\sigma$: $e^{\frac{1}{\sigma^2} \Re \bar{\hat{y}}_j[k] \hat{f}[k] e^{-ik\theta}} = 1 + \frac{\Re \bar{\hat{y}}_j[k] \hat{f}[k] e^{-ik\theta}}{\sigma^2} + R_2\left(\frac{\hat{f}[k]}{\sigma}\right)$, where $R_2(\cdot)$ is the Lagrange remainder. Thus, we can proceed to write the log-likelihood as

$$\begin{aligned} \ell(\hat{f}[k]) &= \sum_{j=1}^n \log C_1 \int_0^{2\pi} e^{C_{j,k}(\theta)} \left(1 + \frac{\Re \bar{\hat{y}}_j[k] \hat{f}[k] e^{-ik\theta}}{\sigma^2} \right. \\ &\quad \left. + R_2\left(\frac{\hat{f}[k]}{\sigma}\right) \right) d\theta \\ &\approx \sum_{j=1}^n \log C_1 \int_0^{2\pi} e^{C_{j,k}(\theta)} \left(1 + \frac{\Re \bar{\hat{y}}_j[k] \hat{f}[k] e^{-ik\theta}}{\sigma^2} \right) d\theta \\ &= \sum_{j=1}^n \log C_1 \left(\hat{C}_{j,k}[0] + \frac{1}{\sigma^2} \Re \bar{\hat{y}}_j[k] \hat{f}[k] \hat{C}_{j,k}[k] \right), \end{aligned} \quad (11)$$

where we defined the Fourier transform of $e^{C_{j,k}(\theta)}$ as:

$$\hat{C}_{j,k}[m] := \int_0^{2\pi} e^{C_{j,k}(\theta)} e^{-im\theta} d\theta. \quad (12)$$

We note that $\hat{C}_{j,k}[m]$ can be computed efficiently with FFT.

Lemma II.1. For $\sigma \rightarrow \infty$, the term inside the log in (11) is strictly positive, i.e., $\hat{C}_{j,k}[0] + \frac{\Re \bar{\hat{y}}_j[k] \hat{f}[k] \hat{C}_{j,k}[k]}{\sigma^2} > 0$.

Proof. For sufficiently large σ , $\hat{y}_j[k]$ scales as σ and thus $|\hat{y}_j[k]| < \sigma^2$. Thus, $1 + \frac{\Re(\bar{\hat{y}}_j[k] \hat{f}[k] e^{-ik\theta})}{\sigma^2}$ is strictly positive. The argument follows since $e^{C_{j,k}(\theta)}$ is also strictly positive, and an integral over a strictly positive function is strictly positive. \square

Next, we use the fact that $\hat{C}_{j,k}[0] \gg \frac{1}{\sigma^2} \Re \bar{\hat{y}}_j[k] \hat{f}[k] \hat{C}_{j,k}[k]$ for $\sigma \rightarrow \infty$, and further expand the log-likelihood using the second-order Taylor expansion $\log(\hat{C}_{j,k}[0] + \frac{\Re \bar{\hat{y}}_j[k] \hat{f}[k] \hat{C}_{j,k}[k]}{\sigma^2}) = \log \hat{C}_{j,k}[0] + \frac{\Re \bar{\hat{y}}_j[k] \hat{f}[k] \hat{C}_{j,k}[k]}{\sigma^2 \hat{C}_{j,k}[0]} + \tilde{R}_2\left(\frac{\hat{f}[k]}{\sigma}\right)$. Therefore,

$$\begin{aligned} \ell(\hat{f}[k]) &= \sum_{j=1}^n \left(\log \hat{C}_{j,k}[0] + \frac{\Re \bar{\hat{y}}_j[k] \hat{f}[k] \hat{C}_{j,k}[k]}{\sigma^2 \hat{C}_{j,k}[0]} \right. \\ &\quad \left. + \tilde{R}_2\left(\frac{\hat{f}[k]}{\sigma}\right) + \log C_1 \right). \end{aligned} \quad (13)$$

The term $\hat{C}_{j,k}[0]$ does not depend on the coefficient $\hat{f}[k]$. Thus, denoting $\hat{f}[k] := |\hat{f}[k]| \phi[k]$, with $|\phi[k]| = 1$, the maximization of the log-likelihood (13) is equivalent (up to high-order terms in the Taylor expansion) to maximizing

$$\sum_{j=1}^n \frac{\Re \bar{\hat{y}}_j[k] |\hat{f}[k]| \phi[k] \hat{C}_{j,k}[k]}{\hat{C}_{j,k}[0]} = |\hat{f}[k]| \Re \phi[k] \sum_{j=1}^n \frac{\bar{\hat{y}}_j[k] \hat{C}_{j,k}[k]}{\hat{C}_{j,k}[0]}. \quad (14)$$

The optimal phase is explicitly given by:

$$\phi^*[k] = \frac{Z}{|Z|}, \quad \text{where } Z = \sum_{j=1}^n \frac{\hat{y}_j[k] \bar{\hat{C}}_{j,k}[k]}{\hat{C}_{j,k}[0]}. \quad (15)$$

This closed-form solution provides the optimal phase for frequency k , conditioned on the current estimates of the remaining frequencies.

Algorithm 1 Fast MLE Algorithm

Input: Observations $\{\hat{y}_j\}_{j=1}^n$, noise variance σ^2 , bandlimit L .
Output: Estimated Fourier coefficients \hat{f} .

Initialize:

- 1: Estimate $\left\{ \widehat{|\hat{f}[k]|} \right\}_{k=1}^L$ according to (6) and $\widehat{\hat{f}[0]}$ according to (5)
- 2: $\hat{f}[1] \leftarrow \widehat{|\hat{f}[1]|}$
- 3: $\hat{f}[k] \leftarrow 0, \forall k \in [2, L]$
- 4: **for** $k = 2$ to L **do**
- 5: **for** $j = 1$ to n **do**
- 6: Compute $\hat{C}_{j,k}$ according to (12)
- 7: **end for**
- 8: Compute optimal phase according to (15) and update the k -th coefficient:
- 9: $\phi[k] \leftarrow Z/|Z|, \hat{f}[k] \leftarrow |\hat{f}[k]|\phi[k]$
- 10: **end for**
- 11: **return** \hat{f}

D. The algorithm

The fast MLE algorithm is summarized in Algorithm 1. First, we estimate the magnitudes of all L coefficients and the zero-frequency coefficient using (6) and (5), respectively. We fix the phase of the $\hat{f}[1]$ to be zero. We initialize the higher frequencies $\hat{f}[k] = 0$ for $k \geq 2$. For each frequency $k \geq 2$, we construct $\hat{C}_{j,k}$ according to (12) using only the previously estimated lower-frequency components ($m < k$), while higher frequencies ($m > k$) are set to zero. Thus, $\hat{C}_{j,k}$ effectively propagates the phase information from the lower spectrum to the current frequency k , guiding its alignment. The k -th coefficient's phase is then updated via the closed-form rule derived from the low-SNR likelihood expansion (15).

Remark II.2. It is worth noting that a simpler “direct” variant of this approach can be also developed. In this formulation, all frequencies are estimated simultaneously, while $\hat{f}[1]$ is fixed to break the symmetry. This corresponds to restricting the alignment kernel to $C_{j,k}(\theta) = \frac{\Re \hat{y}_j[1] \hat{f}[1] e^{-i\theta}}{\sigma^2}$. However, numerical evaluations indicated that this direct approach yields reduced estimation accuracy compared to the frequency marching scheme, and given that the computational speedup offered by the direct method was negligible, we focus exclusively on the frequency marching algorithm.

E. Expectation-Maximization (EM)

EM is the current leading approach for computing the MLE for the MRA problem, particularly in applications like cryo-EM [17], [23]. We introduce it here for comparison to our fast MLE algorithm, as it serves as the state-of-the-art benchmark for this task. The MLE problem is formulated by maximizing the likelihood function over the group of rotations $\text{SO}(2)$. The marginalization over the latent variable—the unknown rotation angles—is done by discretizing the domain of possible rotation angles $[0, 2\pi)$ into a uniform grid of R points, $\Theta_R = \{\theta_r = \frac{2\pi r}{R}\}_{r=0}^{R-1}$. Let $\hat{f}^{(t)}$ denote the estimate of the signal at iteration t . The algorithm alternates between two steps: the expectation step (E-step) and the maximization step (M-step). In the E-step, we estimate the posterior probability distribution of the

rotations. For the j -th observation and grid point θ_r , the weight is calculated as:

$$w_j^{(t)}(\theta_r) = \frac{e^{-\frac{1}{2\sigma^2} \|\hat{y}_j - \sum_{k=0}^L \hat{f}^{(t)}[k] e^{-ik\theta_r}\|^2}}{\sum_{l=0}^{R-1} e^{-\frac{1}{2\sigma^2} \|\hat{y}_j - \sum_{k=0}^L \hat{f}^{(t)}[k] e^{-ik\theta_l}\|^2}}, \quad (16)$$

such that $\sum_r w_j^{(t)}(\theta_r) = 1$. In the M-step, we update the signal estimate by maximizing the expected log-likelihood. This results in a weighted average of the aligned observations:

$$\hat{f}^{(t+1)}[k] = \frac{1}{n} \sum_{j=1}^n \hat{y}_j[k] \left(\sum_{r=0}^{R-1} w_j^{(t)}(\theta_r) e^{ik\theta_r} \right). \quad (17)$$

III. COMPUTATIONAL COMPLEXITY

Let n be the number of measurements and L be the bandlimit. To account for the different discretization requirements, we define R_{EM} - the search grid size for the EM algorithm, and R_{MLE} - the integration grid size for the proposed fast MLE algorithm. Our fast MLE algorithm estimates the coefficient with a total complexity of $\mathcal{O}(n \cdot L^2 \cdot R_{\text{MLE}})$. The magnitudes estimation involves averaging over the set of measurements for each frequency, for a total of $\mathcal{O}(n \cdot L)$ operations. The algorithm then proceeds to estimate the coefficients sequentially. For each frequency $k \in [2, L]$, we sum the contributions of the k previously estimated frequencies, involving an operation of size $(n \cdot k \cdot R_{\text{MLE}})$. Integration involves an FFT over the integration grid R_{MLE} . The dominant cost is the cumulative summation $\sum_{k=2}^L (n \cdot k \cdot R_{\text{MLE}}) \approx \frac{1}{2} n L^2 R_{\text{MLE}}$. The standard EM algorithm performs iterative refinement. The E-Step calculates weights by (16) for n observations over R_{EM} rotations with cost $\mathcal{O}(n \cdot L \cdot R_{\text{EM}})$. The M-Step updates the estimate by averaging the aligned observations with cost: $\mathcal{O}(n \cdot L \cdot R_{\text{EM}})$. The total complexity for T_{EM} iterations is $\mathcal{O}(T_{\text{EM}} \cdot n \cdot L \cdot R_{\text{EM}})$.

A comparison of the computational complexities reveals a trade-off: our fast MLE algorithm scales quadratically with the bandlimit, whereas EM scales linearly per iteration. However, the critical differentiator is the number of iterations, T_{EM} . While our algorithm is a single-pass, closed-form solution with a fixed runtime independent of the noise level, standard EM requires iterative convergence. Crucially, T_{EM} is not constant; it grows very rapidly as the SNR decreases, as can be seen in our numerical experiments in Section IV, and in [13], [20], for instance. In the low-SNR regime, where $T_{\text{EM}} \gg L$, our non-iterative approach offers a substantial computational advantage.

IV. NUMERICAL EXPERIMENTS

We evaluate the performance of the proposed fast MLE algorithm against the standard EM algorithm, initialized from a random initialization point or initialized from the estimation of our algorithm. We generated real bandlimited signals with a bandlimit of $L = 5$; specifically, the real and imaginary parts of the Fourier coefficients were drawn independently from a standard normal distribution, subject to conjugate symmetry constraints. The observations were generated according to the model in (4), with rotation angles drawn uniformly from $[0, 2\pi)$ and additive white Gaussian noise with zero mean and variance σ^2 . For the EM algorithm, we used a discretization grid of $R_{\text{EM}} = 1000$ points, and set a convergence tolerance of 10^{-6} . For the proposed fast MLE algorithm, we used an integration

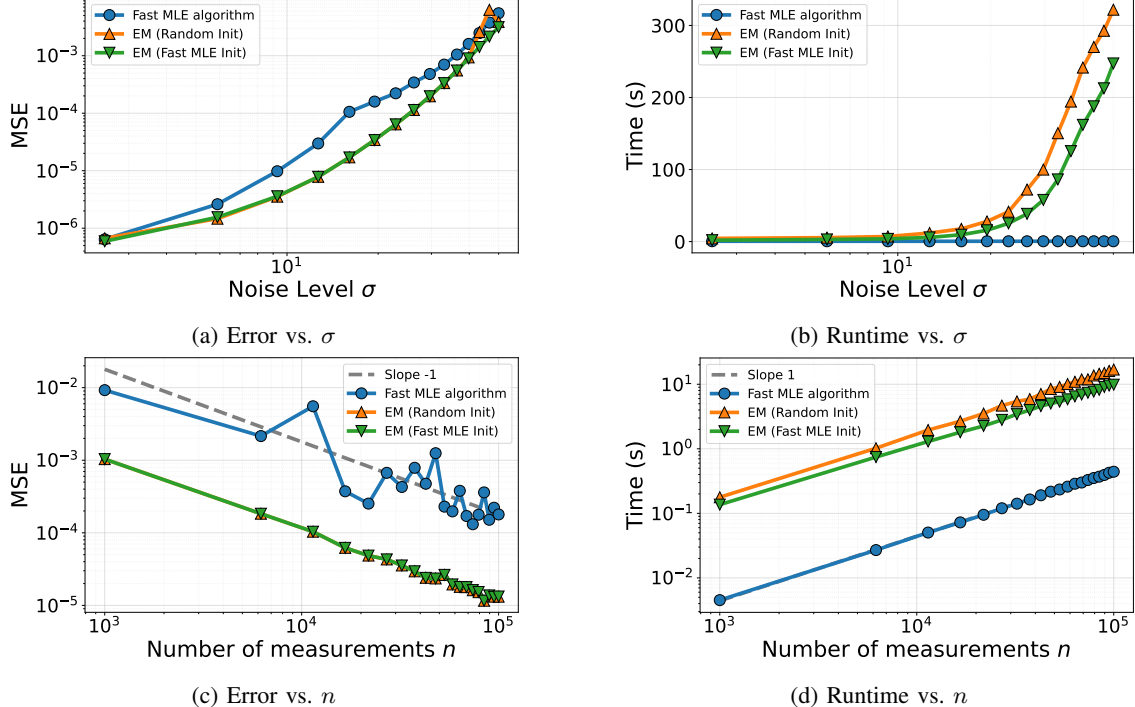


Fig. 1: Performance comparison of the proposed fast MLE algorithm and standard EM, initialized from a random guess or from the result of the fast MLE algorithm. Panels a, b: Comparison of reconstruction error (a) and runtime (b) versus noise level σ , with fixed number of observations $n = 100,000$. The proposed fast MLE algorithm maintains a constant, low runtime regardless of noise intensity. While the EM algorithm achieves lower reconstruction error, it is orders of magnitude slower. Notably, EM initialized with our method outperforms random initialization in low-noise regimes. Panels c, d: Comparison of accuracy (c) and runtime (d) for varying number of observations n , with fixed noise level $\sigma = 12$. Both algorithms exhibit the expected $1/n$ error decay. The results highlight a trade-off: our algorithm offers a dramatic reduction in computational cost with only a small difference in accuracy relative to EM.

grid of $R_{\text{MLE}} = 500$ points. All computations were performed on a MacBook Pro with an Apple M3 Pro chip and 36 GB of RAM. The code to reproduce all numerical experiments is publicly available².

We evaluate the reconstruction accuracy using the mean squared error (MSE) of the Fourier coefficients. Both algorithms recover the signal up to a global rotation α , so we first align the estimate to the ground truth. We search for the optimal shift α^* in a set of shifts that minimizes the ℓ_2 distance between the estimated and true signals. The MSE is then computed as $\text{MSE} = \sum_{k=0}^L \frac{|\hat{f}[k]e^{-ik\alpha^*} - \hat{f}[k]|^2}{|\hat{f}[k]|^2}$, where \hat{f} is the estimated vector of coefficients and \hat{f} is the ground truth.

Figures 1a and 1b compare the estimation error and runtime of both algorithms as a function of the noise level σ . We fixed the number of measurements at $n = 100,000$, and capped the number of EM iterations to 500. The errors were averaged over 10 trials. As shown in Figure 1a, the proposed algorithm achieves competitive reconstruction error compared to EM. Notably, the EM algorithm initialized with our fast MLE method outperforms random initialization. Figure 1b highlights the computational advantage: the runtime of the proposed method is constant with the noise and orders of magnitude lower than EM. EM runtime substantially increases with noise because it requires more iterations to satisfy the convergence

tolerance in low-SNR regimes.

Figures 1c and 1d present the performance as a function of the number of measurements n , with the noise level fixed at $\sigma = 12$. We capped the number of EM iterations to 20, and averaged the errors over 50 trials. The results confirm that both methods exhibit the expected error decay rate of $1/n$ due to the law of large numbers, and also that the computational complexity of both algorithms scales linearly with n . The fast MLE algorithm maintains a stable runtime advantage over the iterative EM approach.

V. A ROADMAP TO FAST MAXIMUM-LIKELIHOOD ESTIMATION FOR CRYO-EM

Our goal is to extend the principles developed in this paper to the full cryo-EM model, which involves 3-D rotations (elements of the group $\text{SO}(3)$) and tomographic projections [11]. In brief, the key idea is to formulate the likelihood in terms of orthogonal matrices (see, e.g., [24]), which play the $\text{SO}(3)$ analog of the Fourier phases in the $\text{SO}(2)$ setting. Using similar Taylor expansions, the resulting MLE reduces to a Procrustes problem, whose solution is obtained via an SVD: mirroring the phase-recovery step used in (15). We leave a complete derivation and an efficient implementation to future work. If realized, this approach could provide an extremely fast *ab initio* estimator, yielding a robust initialization for standard cryo-EM pipelines.

²Code available at <https://github.com/krshay/Fast-MLE-MRA-SO2>.

REFERENCES

- [1] J. Frank, *Three-dimensional electron microscopy of macromolecular assemblies: Visualization of biological molecules in their native state*. Oxford University Press, 2006.
- [2] M. Irani and P. Anandan, “Robust multi-sensor image alignment,” in *Sixth International Conference on Computer Vision*. IEEE, 1998, pp. 959–966.
- [3] A. Singer, “Angular synchronization by eigenvectors and semidefinite programming,” *Applied and Computational Harmonic Analysis*, vol. 30, no. 1, pp. 20–36, 2011.
- [4] A. S. Bandeira, M. Charikar, A. Singer, and A. Zhu, “Multireference alignment using semidefinite programming,” in *Proceedings of the 5th Conference on Innovations in Theoretical Computer Science*, 2014, pp. 459–470.
- [5] T. Bendory, N. Boumal, C. Ma, Z. Zhao, and A. Singer, “Bispectrum inversion with application to multireference alignment,” *IEEE Transactions on Signal Processing*, vol. 66, no. 4, pp. 1037–1050, 2017.
- [6] X.-C. Bai, G. McMullan, and S. H. Scheres, “How cryo-EM is revolutionizing structural biology,” *Trends in Biochemical Sciences*, vol. 40, no. 1, pp. 49–57, 2015.
- [7] E. Nogales, “The development of cryo-EM into a mainstream structural biology technique,” *Nature Methods*, vol. 13, no. 1, pp. 24–27, 2016.
- [8] K. M. Yip, N. Fischer, E. Paknia, A. Chari, and H. Stark, “Atomic-resolution protein structure determination by cryo-EM,” *Nature*, vol. 587, no. 7832, pp. 157–161, 2020.
- [9] F. J. Sigworth, “Principles of cryo-EM single-particle image processing,” *Microscopy*, vol. 65, no. 1, pp. 57–67, 2016.
- [10] A. Singer and F. J. Sigworth, “Computational methods for single-particle electron cryomicroscopy,” *Annual Review of Biomedical Data Science*, vol. 3, pp. 163–190, 2020.
- [11] T. Bendory, A. Bartesaghi, and A. Singer, “Single-particle cryo-electron microscopy: Mathematical theory, computational challenges, and opportunities,” *IEEE Signal Processing Magazine*, vol. 37, no. 2, pp. 58–76, 2020.
- [12] A. S. Bandeira, B. Blum-Smith, J. Kileel, J. Niles-Weed, A. Perry, and A. S. Wein, “Estimation under group actions: recovering orbits from invariants,” *Applied and Computational Harmonic Analysis*, vol. 66, pp. 236–319, 2023.
- [13] N. Janco and T. Bendory, “An accelerated expectation-maximization algorithm for multi-reference alignment,” *IEEE Transactions on Signal Processing*, vol. 70, pp. 3237–3248, 2022.
- [14] A. S. Bandeira, J. Niles-Weed, and P. Rigollet, “Optimal rates of estimation for multi-reference alignment,” *Mathematical Statistics and Learning*, vol. 2, no. 1, pp. 25–75, 2020.
- [15] A. Perry, J. Weed, A. S. Bandeira, P. Rigollet, and A. Singer, “The sample complexity of multireference alignment,” *SIAM Journal on Mathematics of Data Science*, vol. 1, no. 3, pp. 497–517, 2019.
- [16] A. P. Dempster, N. M. Laird, and D. B. Rubin, “Maximum likelihood from incomplete data via the EM algorithm,” *Journal of the Royal Statistical Society: Series B (Methodological)*, vol. 39, no. 1, pp. 1–22, 1977.
- [17] F. J. Sigworth, “A maximum-likelihood approach to single-particle image refinement,” *Journal of Structural Biology*, vol. 122, no. 3, pp. 328–339, 1998.
- [18] Z. Fan, Y. Sun, T. Wang, and Y. Wu, “Likelihood landscape and maximum likelihood estimation for the discrete orbit recovery model,” *Communications on Pure and Applied Mathematics*, vol. 76, no. 6, pp. 1208–1302, 2023.
- [19] Z. Fan, R. R. Lederman, Y. Sun, T. Wang, and S. Xu, “Maximum likelihood for high-noise group orbit estimation and single-particle cryo-EM,” *The Annals of Statistics*, vol. 52, no. 1, pp. 52–77, 2024.
- [20] A. Balanov, W. Huleihel, and T. Bendory, “Expectation-maximization for multi-reference alignment: Two pitfalls and one remedy,” *arXiv preprint arXiv:2505.21435*, 2025.
- [21] T. Bendory, N. Boumal, W. Leeb, E. Levin, and A. Singer, “Toward single particle reconstruction without particle picking: Breaking the detection limit,” *SIAM Journal on Imaging Sciences*, vol. 16, no. 2, pp. 886–910, 2023.
- [22] T. Bendory, D. Edidin, J. Katz, and S. Kreymer, “Orbit recovery for spherical functions,” *arXiv preprint arXiv:2508.02674*, 2025.
- [23] S. H. Scheres, “RELiON: implementation of a Bayesian approach to cryo-EM structure determination,” *Journal of Structural Biology*, vol. 180, no. 3, pp. 519–530, 2012.
- [24] T. Bendory and D. Edidin, “The sample complexity of sparse multireference alignment and single-particle cryo-electron microscopy,” *SIAM Journal on Mathematics of Data Science*, vol. 6, no. 2, pp. 254–282, 2024.